THE ASTROPHYSICAL JOURNAL, 472:294–307, 1996 November 20

THE *IUE* SPECTRUM OF THE PLANETARY NEBULA NGC 6905

WALTER A. FEIBELMAN[1]
Laboratory for Astronomy and Solar Physics, Code 681, NASA Goddard Space Flight Center, Greenbelt, MD 20771; feibelman@stars.gsfc.nasa.gov
Received 1996 March 7; accepted 1996 June 6

ABSTRACT

We present results from new *IUE* high-dispersion and archival low-dispersion spectra of NGC 6905. Ultraviolet emission lines of O VIII and possibly O VII are detected for the first time in NGC 6905. High-excitation lines of C IV, C V, O VI, [Mg V], [Ne III], [Ne IV], [Ne V], [Ar IV], and [Ar V] are also observed. Electron densities and terminal wind velocities are presented. Terminal wind velocities from O V and C IV lines are discussed. Variability (up to ≈25%) of the complex split He II λ1640 emission may be intrinsic or a function of position angle of the *IUE* camera entrance aperture. After reextracting the low-dispersion data, no significant changes between 1981 and 1991 were found for the strong O V λ1371, C IV λ1549, He II λ1640, and C III] λ1909 emissions. Many weak features not detected before have been identified in the archival low-resolution data. Some comparisons are made with UV spectra of Sand 3 and KPD 0005+6501. Preliminary results indicate O VIII emissions in *IUE* spectra of NGC 2371-2, NGC 2867, NGC 5189, and NGC 5315, suggesting that these planetary nebulae, together with NGC 6905, RX J2117+3412, and Sand 3, form a new "O VIII sequence." The present work illustrates the need to reexamine older *IUE* spectra and demonstrates that today's improved data analysis is capable of improving greatly the results reported in earlier publications.

Subject headings: planetary nebulae: individual (NGC 6905) — ultraviolet: ISM

1. INTRODUCTION

The variable planetary nebula (PN) NGC 6905 (061.4−09.5 in the notation of Acker et al. 1992, hereafter A92) has been studied extensively, but its ultraviolet characteristics have received relatively little attention. The *IUE* low-dispersion spectrum of NGC 6905 was described by Johnson (1981, hereafter J81). Feibelman (1982, hereafter F82) searched for variability in *IUE* spectra and showed stratification effects for different emissions from echelle line-by-line analysis (the new data for the peculiar asymmetric He II emission are discussed further in § 4.2.3). In a survey of about a dozen O VI central stars, Bianchi (1989, hereafter B89) derived the interstellar extinction $E(B-V) = 0.15$ from the λ2200 bump, as well as some other parameters.

The optical spectrum of NGC 6905 was studied in detail by Aller (1951, 1968), who also observed the object in the red and near-infrared region (Aller 1977). Swings & Swensson (1952) commented on the strength of the He II λ4686 line, comparable to Hβ. The broad Wolf-Rayet emissions were depicted by Aller (1968) and show the narrow nebular emissions superposed on broad stellar features. NGC 6905 belongs to the small group of very high excitation PNs that exhibit very strong emission lines of O VI near λλ3811, 3834, the so-called O VI sequence defined by Smith & Aller (1969). Only about two dozen objects of this type are known, and some exhibit variability. Variability for NGC 6905 was demonstrated by Vorontsov-Velyaminov (1961, hereafter VV61) on the basis of a change in the stellar He II λ4686/Hβ intensity ratio from a value of 0.5 to 1.3 between the years 1945 and 1959. Optical spectra do not display P Cyg profiles, but the UV data show strong P Cyg profiles for C IV and O V, while N V is very weak and its reality is doubtful. Similarly, the N III] λ1750 multiplet is weak, which suggests that NGC 6905 is nitrogen poor.

Radial velocities for several O VI PNs were measured first by D'Odorico, Rubin, & Ford (1973) but differ from that given by A92 (−7.4 km s^{-1}) for NGC 6905, based on radio observations from Schneider et al. (1983). D'Odorico et al. also measured the He II λ4686 intensity as 102 on a scale of I(Hβ) = 100.

Expansion velocity field maps, derived from spectra taken at different slit position angles of NGC 6905, were presented by Sabbadin & Hamzaoglu (1982, hereafter SH82). All emission lines show splitting, and the [O III] λ5007 emission gives a peak-to-peak value of ∼100 km s^{-1}, depending on position angle. A slightly smaller value was obtained for Hα. The systemic radial velocity given by SH82 is −10 km s^{-1}. These velocities are important to the discussion of *IUE* data in § 4.2.3.

Kaler & Shaw (1984, hereafter KS84) listed several parameters for NGC 6905, including a $T_{\rm eff} = 104{,}000$ K that is comparable with the other O VI planetary nebula nuclei (PNNs) of their study and is considerably higher than the 50,000 K given by B89, or the 60,000 K derived by J81 from *IUE* data. They also gave an intensity $I = 98$ for the He II λ4686 emission, compared to $I = 100$ for Hβ. NGC 6905 has the distinction of having the greatest optical O VI λλ3811, 3834 equivalent width, 700 Å, of any of the stars measured by KS84.

Stanghellini et al. (1995, hereafter SKSD95) measured optical emission lines and located NGC 6905 on the H-R plane of log $T_{\rm eff}$, $L/L_\odot$ for comparison with a dozen other "O VI sequence" PNNs and also commented on the strength of [Ne III] lines. Their value of interstellar extinction, $c = 0.93$, is much higher than that inferred by B89 from the UV λ2200 extinction bump.

A set of four monochromatic CCD images of the nebula and star was presented by Balick (1987) and are reproduced in A92, superseding earlier photographic images by Louise (1982) and Louise & Hua (1984), as well as two CCD Hα

[1] Guest Observer with the *International Ultraviolet Observer* (*IUE*) satellite, which is sponsored and operated by the National Aeronautics and Space Administration, by the European Space Agency, and by the Science and Research Council of the United Kingdom.

images by Chu, Jacoby, & Arendt (1987). The remarkably complex structure first reported by Curtis (1918) from visual sketches and photographs is confirmed by the modern images.

Nonradial g-mode pulsation periods of about 16 minutes for the central star were reported by Bond & Ciardullo (1990, 1993) and Bond, Ciardullo, & Kawaler (1993). These were confirmed by Silvotti et al. (1993), who gave principal periods of 12.9 and 17.6 minutes. The most recent study by Ciardullo & Bond (1996) indicates pronounced variations in light curves and power spectra for NGC 6905.

A detailed model of the nebula and its conical ansae was presented by Cuesta, Phillips, & Mampaso (1993, hereafter CPM93). In an earlier work, Phillips & Mampaso (1989, hereafter PM89) mention that the central star of NGC 6905 is a binary whose separation is $3''.6$, but this proved to be erroneous, and the nucleus is a single star (A. Mampaso, private communication).

Tarafdar & Apparao (1988) list NGC 6905 as a possible X-ray source for which they gave only an upper limit of detection, as observed with the *Einstein* satellite. The central star shares some of the UV characteristics observed in confirmed X-ray PNs, namely, P Cyg profiles that imply strong stellar winds, and a C IV λ1549/He II λ1640 ratio greater than 1 (Feibelman 1994).

The present study is concerned with the bright main body of the nebula and its central star but ignores the outer, faint ansae. We demonstrate that NGC 6905 presents an extremely complex UV spectrum and identify very high excitation emission lines from new *IUE* high-dispersion spectra. and we determine electron densities and terminal wind velocity. The detection of O VIII emission features makes NGC 6905 the third member of a select group that may constitute an "O VIII sequence" of planetaries and suggests that NGC 6905 is an object worthy of further study.

2. OBSERVATIONS

The *IUE* archive contains 11 low-dispersion spectra and one (relatively short, 120 minute) short-wavelength prime (SWP) high-dispesion spectrum. Two deep SWP and the first long-wavelength prime (LWP) high-dispersion spectrum were obtained by the writer in 1995. The *IUE* Log of Observations for NGC 6905 is summarized in Table 1. This shows the image sequence number in column (1); low or high dispersion in column (2); the date of observation in column (3); the exposure time in minutes in column (4); the space craft roll (SCR) angle in column (5); the position angle of the major axis of the large ($10'' \times 23''$) entrance aperture in column (6); ad some comments in column (7).

The position angle (P.A.) refers to that of the major axis of the large entrance aperture and is determined from the space craft roll (SCR) angle. The P.A. = 73° minus SCR angle. See NASA *IUE* Newsletter 47 (1992) for further details. All observations were taken through the large entrance aperture of the *IUE* cameras and were centered on the nucleus of the PN. The data were reduced by means of the interactive computer routines available to guest observers at the Goddard Data Analysis Center (IUEDAC) and made use of the most recent calibration procedures.

3. WAVELENGTH IDENTIFICATIONS

We rely on several sources for wavelength identifications. These include Aller (1951, 1968, hereafter A51 and A68, respectively, Kelly (1979, hereafter K79), Kurucz (1991, hereafter K91), Morton (1991, hereafter M91), Moore (1993, hereafter M93), Doschek & Feibelman (1993, hereafter DF93), Feibelman & Johansson (1995, hereafter FJ95), and Garcia & Mack (1965).

For the He II wavelength identifications we rely on air rest wavelengths given by K79: $\lambda\lambda$(2252.689), 2511.205, (2306.195), (2385.404), 2733.297, and 3203.102. We adhere to these values for consistency of plotting the stronger lines (shown without parentheses) in velocity space (see § 4.2.3), although slightly different values can be found in the literature.

The [Ne V] line at 1980 Å identified by Barlow & Hummer (1982) in the *IUE* spectrum of Sand 3 is now given by K91 at 1989 Å; however, three unidentified features are resolved at λ1980 in high-dispersion data.

TABLE 1

LOG OF *IUE* OBSERVATIONS FOR NGC 6905

Image Sequence Number: SWP (1)	Image Sequence Number: LWP/LWR (1)	Dispersion (2)	Date (3)	Exposure (minutes) (4)	SCR Angle[a] (deg) (5)	Position Angle (deg) (6)	Comments (7)
02228		Low	1978 Aug 7	20	18	+55	
	02006	Low	1978 Aug 7	20	18	+55	
13404		Low	1981 Mar 4	90	239	−166	Saturated (<1400 Å, C IV, He II, C III saturated)
13405		Low	1981 Mar 4	20	239	−166	
	10067	Low	1981 Mar 4	100	239	−166	Saturated
	10068	Low	1981 Mar 4	20	239	−166	
	14401	Low	1981 Jul 5	30	333	−260	
	11012	Low	1981 Jul 5	30	333	−260	
16703		Low	1982 Apr 6	25	269	−196	C IV slightly saturated[b]
	12969	Low	1982 Apr 6	25	269	−196	$\lambda\lambda$2783–2800 saturated
18366		High	1982 Oct 22	200	97	−24	Not saturated
41863		Low	1991 Jun 18	30	17	+56	Not saturated[c]
	31209	High	1995 Aug 12	488	11	+62	Not saturated
55994		High	1995 Sep 23	405	76	−3	C III] saturated
56067		High	1995 Oct 10	532	89	−16	C III] saturated

[a] Spacecraft roll angle is rounded off to nearest degree.
[b] High radiation background.
[c] Cosmic radiation hit may affect He II λ1640 line.

4. DISPERSION

4.1. *The Low-Dispersion Data*

The *IUE* low-dispersion data were discussed by J81, F82, and B89, who identified only about two dozen emission features. Considerably more information can be extracted now from these early spectra by means of the improved data reduction techniques that have been developed during the past 18 years at the Goddard Data Analysis Center (IUEDAC). In the SWP region alone, more than 35 features are measurable, compared to only 12 lines, or blends of lines, listed by J81 and F82. In Figure 1 we show the newer archival SWP 41863 of 30 minutes exposure after it was reextracted as described in § 4.1. On this figure, and all subsequent figures, the vertical scale shown is in units of ergs cm^{-2} s^{-1} A^{-1}.

The LWR 10067 spectrum is shown in Figure 2. Although saturated, this spectrum is very useful to show weak features that are not detected on shorter exposures.

In Figure 3 we show the region λλ2000–2400 of NGC 6905, which is similar to that of the ultra-high excitation low-mass W-R star Sand 3, considered to be a remnant central star without a detectable PN; see Barlow & Hummer (1982, hereafter BH82) and Feibelman (1996a, hereafter F96a) for further details. The region contains emission lines of O VI λ2070, [Ne V] λλ2236, 2250, He II λ2252, and C V λλ2270, 2277. Additional similarities of the two objects are discussed in § 4.2.

We take this opportunity to advise caution in accepting data from the "final archive" at face value. Probably the vast majority of these data for stellar objects are trust-

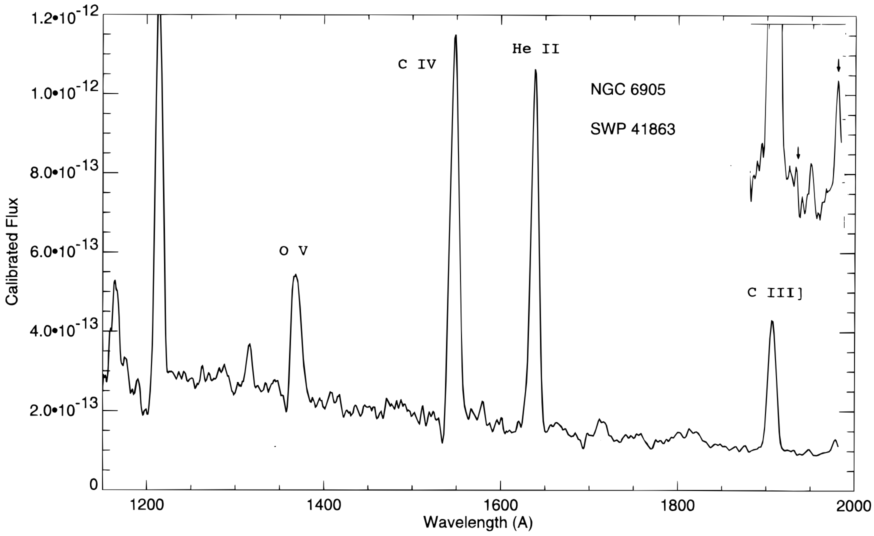

FIG. 1.—The low-dispersion SWP spectrum of NGC 6905 covering the range λλ1150–2000. This is the reprocessed archival image SWP 41863, 30 minute exposure without saturation. Arrows point toward the weak emission lines near 1930 and 1980 Å shown enlarged in the inset. The feature at 1930 Å is interpreted as due to O VIII, and near λ1980 emission is [Ne V] λ1989 from Kurucz (1991), formerly thought to be at 1980 Å (Barlow et al. 1980). On this figure, as well as all others, the vertical scale is in units of ergs cm^{-2} s^{-1} $Å^{-1}$.

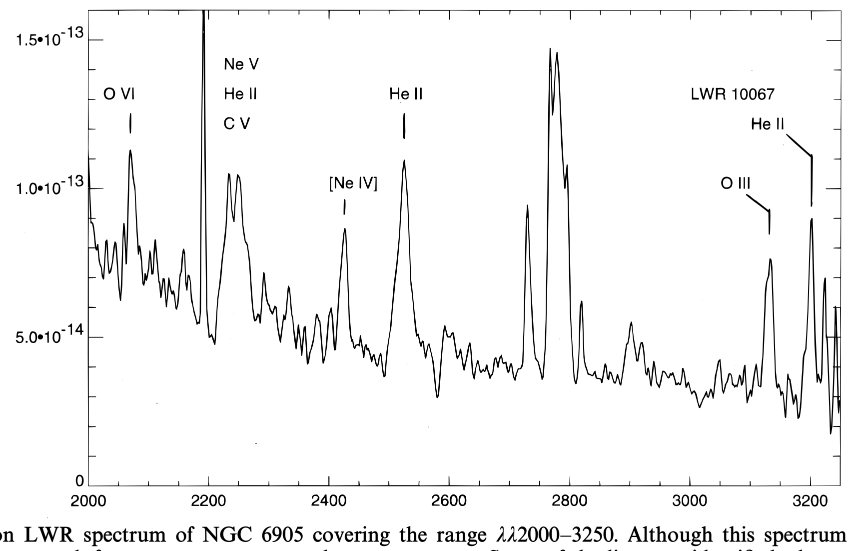

FIG. 2.—The low-dispersion LWR spectrum of NGC 6905 covering the range λλ2000–3250. Although this spectrum (LWR 10067, 100 minutes) is saturated, it is shown to indicate weak features not present on shorter exposures. Some of the lines are identified; the emission labeled He II at 2511 Å contains several C IV components shown in Tables 2 and 4. The large emission feature near 2800 Å is shown in detail in Figure 4 from high-resolution data.

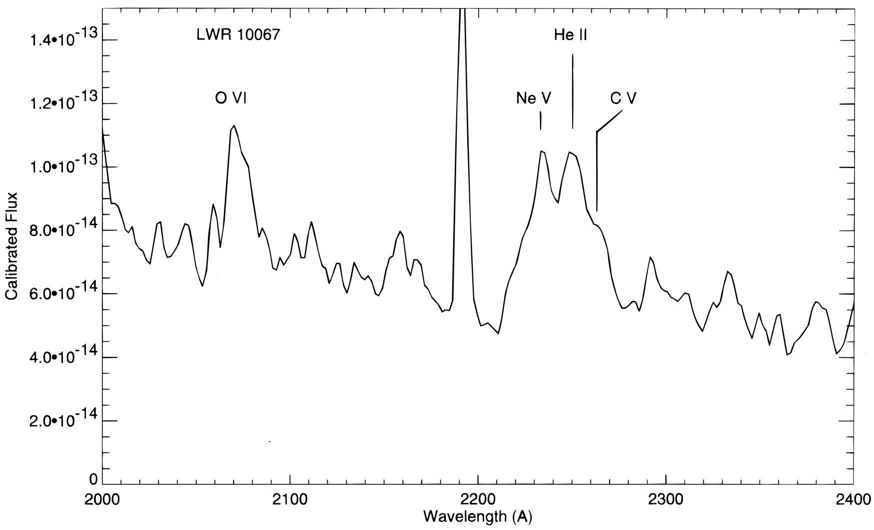

FIG. 3.—The region $\lambda\lambda$2000–2400 from LWR 10067. Emission lines of O VI, [Ne V], C IV, He II, and C V are indicated. As can be seen from Table 4, at least seven [Ne V] and two Fe II emissions are resolved in the high-dispersion spectrum.

worthy, yet caution must be exercised for spectra of extended objects and for exposures affected by cosmic radiation hits. Comparison of the three best unsaturated SWP spectra, 14401, 16703, and 41863, revealed an apparent dramatic change in the He II λ1640 emission: a drop of almost 50% in the emission flux for SWP 41863 compared to the other spectra. After some time was spent trying to verify this change (which occurred for the λ1640 line only), it became clear that the reprocessed SWP.mxlo file used the automatic routine SWET (signal weighted extraction technique) that eliminates blemishes and cosmic radiation hits. However, this method may overcorrect and throw away good data in the process, as it did for SWP 41863. Furthermore, the spectrum was not as well centered in the aperture as the others. Therefore, it is mandatory to examine the line-by-line file and reextract the data by means of the routine BOXCAR to integrate all echelle lines that contain useful information. Thus, it was found that He II λ1640 emission is of stellar and nebular origin and extends from echelle line 43 to 72. Because of a nearby cosmic-ray hit, much of the data was deleted by the routine SWET, resulting in a flux that was about half its true value. When the flux is measured for the full range of integration, its value is the same (within an error of $\pm 10\%$) as for SWP 13401 or SWP 16703. A more detailed description can be found in NASA *IUE* Newsletter 56 (1996); see also Nichols & Linsky (1996).

In Table 2A we present the observed wavelengths from SWP 41863 in column (1); the laboratory rest wavelengths in column (2); the ion identification in column (3); the source of identification in column (4); the remeasured emission-line fluxes (not corrected for extinction) from the best four spectra in columns (5), (6), (7), and (8); and some comments in column (9). The strong lines are heavily saturated in SWP 13404, but this spectrum is useful for detection of the weaker lines.

Table 2B contains similar information from LWR data. LWR 10067 is used for the weak lines, although the stronger lines are heavily saturated in this spectrum. Many high-excitation emission lines of C IV, C V, O III, [Ne V], and [Mg V] are present in the UV spectrum of NGC 6905 and its central star. Footnote b in Table 2 corresponds to lines that were detected in high-dispersion data whose wavelength determinations are much superior to those from final archive low resolution, the reverse is true for flux measurements because final calibrations for high-dispersion spectra are not yet available.

4.2. *The High-Dispersion Data*

Apparently no detailed discussion of the SWP 18366 spectrum has been published so far. The new SWP 55994, SWP 56067, and LWP 31209 spectra were obtained during 1995.

The LWP spectrum of NGC 6905 resembles that of Sand 3 in that the region $\lambda\lambda$2750–2810 is crowded with numerous emission features that are difficult to resolve (see F96a). Moreover, until recently Sand 3 was thought to be a unique object with ultra–high excitation lines of O VIII (IP = 871.4 eV) in the optical region but has been joined by objects like KPD 0005 + 5106, RX J2117 + 3412, and others (see Werner et al. 1996, and references therein). We report the first detection of the ultraviolet emission lines of O VIII near 1930 Å and 2976 Å for NGC 6905 in § 4.2.5.

Emission features that fall within a fraction of an angstrom of known transitions for the crowded region $\lambda\lambda$2750–2870 are identified in Table 3, but definite identification and flux measurements require higher signal-to-noise (S/N) data. Isolated measurable lines are listed in Table 4. We show a section of the LWP 31209 spectrum in Figure 4 to indicate the richness of [Ne V] lines and for comparison with the low-resolution Figure 3. A smoothed plot of the regions $\lambda\lambda$2755–2805 is shown in Figure 5, where some rest wavelengths of likely identifications are indicated. This plot is shown primarily as guidance for future investigations, as the region is too crowded for *IUE* to resolve individual lines. Moreover, it is impossible to determine the level of the continuum for this wavelength region.

4.2.1. *Terminal Wind Velocities*

The signal-to-noise ratio (S/N) for the three co-added high-dispersion spectra is too low to determine a valid P Cyg profile for the C IV doublet, even though it is seen on all low-dispersion spectra. Therefore, we, rely on the mean of the three best (not saturated) low-resolution spectra for a determination of $V_\infty = -3880 \pm 200$ km s^{-1} as shown in

TABLE 2

EMISSION-LINE FLUXES FROM LOW-DISPERSION SPECTRA

A. SWP RANGE

λ(obs) (Å) (1)	λ(lab) (Å) (2)	ION (3)	REFERENCE (4)	FLUX (10^{-13} ergs cm^{-2} s^{-1}) 41863[a] (5)	16703[a] (6)	14401[a] (7)	13404[a] (8)	REMARKS (9)
1165.46......	1168.99[b]	C IV	1	(16.71)	...	(42.06)	(35.95)	
1175.84......	1175.50[b]	C III	2	1.26	...	3.79:	...	Blend
1189.85......	1184/91[b]	C IV, O VI	1	0.96	...	...	...	Blend
1241.99......	1239/42	N V	3	0.58	2.98	2.18	...	Blend
1262.99......	1261/62	O VI	1	1.59	2.25	1.42	...	Blend
1270.41......	1268.99	C IV	1	0.9	...	...	...	
1287.61......	1289/91[b]	O V	1	1.56	5.37	0.66	5.63	Blend
1291.51......	1293.90[b]	[Mg V]	4	3.07	1.37	1.12	2.91	
1315.28......	1315.85[b]	C IV	1	8.21	14.22	7.71	9.19	
1325.76......	1324.50[b]	[Mg V]	4	2.20	2.44	1.42	3.24	
1344.32......	1344.41	C IV	1	...	...	1.16	...	Blend
1350.14......	1351/52	C IV	1	2.64	10.97	2.98	4.16	
1369.41......	1371.29[b]	O V	5	41.55	42.24	41.45	>41.26	
1395.04......	1393/96	Si IV, O IV	2	1.36	...	...	...	Blend
1407.35......	1407.38	O IV	2	2.74	4.3	1.06	...	
1416.11......	1413.39	O VI	1	1.76	3.93	0.93	...	
1436.32......	1440.36[b]	C IV	1	1.58	1.78	1.61:	0.83	
1451.23......	...	?		3.63	3.21	...	...	
1511.70......	1506.71	C IV	5	1.62	1.93	1.08:	...	
1547.76......	1549/52[b]	C IV	3	109.60	>122.23	111.30	>104.00	Blend
1579.02......	1575/76[b]	[Ne V]	4	2.53	5.79	0.85:	1.29	+C III
1595.42......	1596.37	C IV	5	1.54	...	...	...	Blend
1600.61......	1601.20	[Ne IV]	6	1.43	...	...	...	
1620.22......	1619.80[b]	C V	5	1.08	1.19	1.00:	...	
1620.38......	1620.33[B]	C III	5	...	...	...	...	Blend 5
1637.91......	1640.39[b]	He II	5	95.87	95.31	92.06	>86.00[c]	
1663.11......	1661/66	O III]	3	3.01	3.31	3.55	3.15	Blend
1710.82......	1707.99	O V	5	2.32	...	1.73	1.21	
1717.33......	1718.55	N IV	2	1.97	1.30	4.06	6.52	
1724.02......	1722.09[b]	[Ne V]	7	...	...	...	0.74	
1756.06......	1749/54[b]	N III]	3	0.85	2.74	2.57	1.56	
1812.91......	1814.69[b]	[Ne III]	2	0.75	1.21	0.41	2.02	Blend
1821.25......	1817.41	Si II	2	0.61	...	0.85	1.60	
1865.17......	1860.98	C IV	1	0.35:	...	1.34:	0.81:	
1875.40......	1874.95	O III	5	0.88:	1.42:	...	0.63:	
1892.34......	1892.04	Si III]	2	0.30:	0.46:	0.34:	...	
1906.58......	1907/09[b]	C III]	3	35.00	32.51	35.69	>32.48	
1931.03......	1930/32[b]	O VIII	5	0.28:	0.76:	0.48:	0.81:	
1947.39......	1949.35	Si II	2	1.10	1.56:	...	...	
1977.61......	1979.62	C III?	5	2.24	1.06:	...	...	

B. LWR RANGE[d]

λ(obs) (Å) (1)	λ(lab) (Å) (2)	ION (3)	REFERENCE (4)	FLUX (10^{-13} ergs cm^{2} s^{-1}) 12696 (5)	11012 (6)	10068 (7)	10067 (8)	REMARKS (9)
2071.08......	2069.92[b]	O VI	5	(6.28)	6.28	15.03	5.92	
2084.90......	2082.18	O IV	5	...	4.60	...	0.97:	
2156.79......	2142/45	O III	5	...	...	4.38	2.02	
2235.94......	2236.30	C IV	5	3.26	5.32	4.31	5.15	Blend
2236.43......	2236.29[b]	[Ne V]	7	...	...	...	...	
2250.45......	2250.00	C IV	5	...	...	...	...	Blend
2253.03......	2252.69[b]	He II	6	9.31	9.33	6.62	6.90	
2268.48......	2271/77[b]	C V	5	...	3.75	2.00	2.39	Blend
2303.09......	2301.94	C IV	5	1.61	3.20:	...	...	
2332.27......	2332.64	S III?	6	9.07	2.76:	2.78	2.09	
2404.48......	2405.10	C IV	5	1.61	...	...	1.11	
2424.68......	2422/24[b]	[Ne IV]	3	7.54	8.85	5.50	5.84	Blend
2511.41......	2511.20[b]	He II	6	1.57	3.85	6.63	4.10	
2524.14......	2524.41[b]	C IV	5	...	...	...	...	
2528.45......	2524.41	C IV	5	...	...	...	...	Blend of 5 lines
2529.98......	2529.98	C IV	5	...	...	...	...	
2532.12......	2530.60[b]	C IV	5	12.80	11.23	14.08	11.31	
2598.38......	2605.00	Fe II	6	4.04	1.17	3.17	1.66	Multiplet
2731.08......	2733.29[b]	He II	6	3.58	5.24	4.48	5.68	
2784.	2783.10[b]	[Mg V]	6	...	...	...	...	

TABLE 2B—*Continued*

λ(obs) (Å) (1)	λ(lab) (Å) (2)	Ion (3)	Reference (4)	Flux (10^{-13} ergs cm^2 s^{-1}) 12696 (5)	11012 (6)	10068 (7)	10067 (8)	Remarks (9)
2786.	2785.99[b]	[Ar v]	6	33.14	>26.43	30.05	>31.81	Sum of 4 lines
2787.	2786.99[b]	O v	6	...	...	...	...	
2802.	2802.70[b]	Mg II	6	...	...	...	...	
2819.06......	2818.24	C IV	5	...	...	...	1.42	
2900.76......	2901.60[b]	C IV	5	1.34	Noise	...	3.05	Blend
2905.00......	2906.29[b]	C IV	5	...	Noise	...	...	
2930.64......	2928.30	[Mg v]	6	3.08	Noise	1.61	0.26:	
2940.07......	2941.65	O v	5	...	Noise	...	0.41	
2974.72......	2974.20[b]	[Ne v]	7	3.26	Noise	1.01	0.20:	
2994.59......	2992/3	[Ne v], O v	6	3.47	Noise	1.94	...	Blend
3047.27......	3047.13[b]	O III	6	3.00	1.08	3.48	1.11	
3133.8	3132.90[b]	O III	6	8.75	9.42	7.45	6.76	
3203.70......	3203.10[b]	He II	6	4.98	9.11	7.60	6.12	
3225.35......	3223.01	Si II?	8	Noise	5.97	8.85	2.43	
3271.97......	3275.63	O v	5, 9	Noise	3.71	4.05	1.43:	

[a] From reextracted files (see § 4.1).
[b] Lines detected in high-resolution spectra.
[c] He II line may be affected by cosmic radiation hit. See § 4.1.
[d] Wavelengths determined from single and deconvolved blended lines of LWR 10067.
References.—(1) Feibelman & Johansson 1995; (2) Doschek & Feibelman 1993; (3) Morton 1991; (4) Mendoza 1983; (5) Moore 1993; (6) Kelly 1979; (7) Kurucz 1991; (8) Adelman, Adelman, & Fischel 1977; (9) Aller 1968, where the O v λ3275 line was observed from the ground.

Figure 6. This is a section from 1500–1675 Å of the unsaturated SWP 41863; the strong C IV and He II lines are shown truncated for better visibility of the P Cyg absorption of the C IV feature. Thus, the terminal wind velocity for NGC 6905 is near the upper limit encountered for PNs by Patriarchi & Perinotto (1991, hereafter PP91).

Low-dispersion spectra also show a P Cyg profile for the O v λ1371 line. The three co-added high dispersion spectra give $V_\infty = -2730 \pm 150$ km s^{-1} for the λ1371 P Cyg profile.

The N v doublet does not exhibit a P Cyg profile in high dispersion, although interstellar λ1238 and λ1242 absorption components are present. The N v doublet is barely detectable in the low-resolution spectra, yet variablity cannot be ruled out.

4.2.2. *Electron Densities*

On first impression, the unsaturated SWP 18366 spectrum yields an approximate electron density, log $N_e = 3.1$ cm^{-3} from the C III] $F(\lambda1907)/F(\lambda1909)$ ratio = 1.44, based on the diagnostic curves of Keenan, Feibelman, & Berrington (1992) and the assumption that all flux is of nebular origin at T = 10,000 K. However, the triple-peaked C III] profiles shown in Figure 7 strongly suggest a contribution from the central star. Therefore, we deconvolved each C III] component into one stellar and two nebular Gaussian profiles and derived separate fluxes. This yields a stellar flux of 6.2×10^{-13} ergs cm^{-2} s^{-1} plus a sum of the nebular contributions equal to 1.3×10^{-12} ergs cm^{-2} s^{-1} for the λ1907 component; similarly, a stellar flux of 2.8×10^{-13} ergs

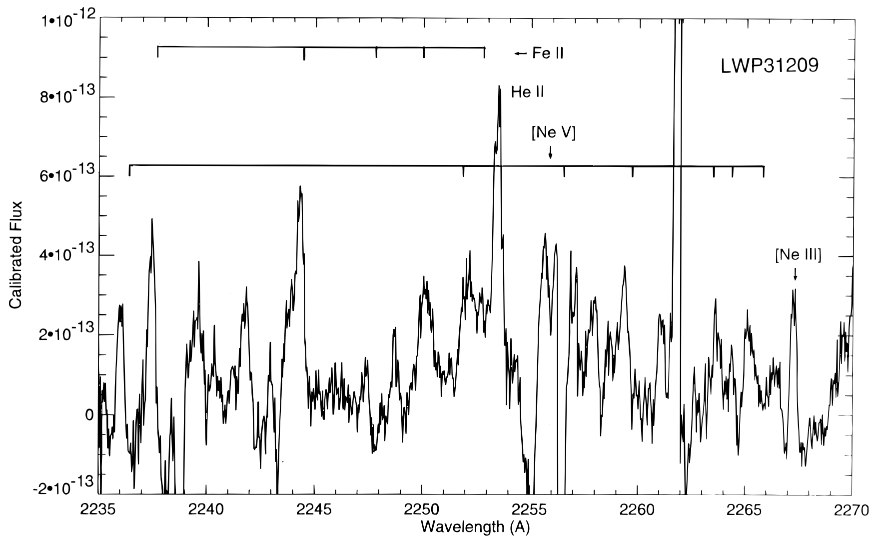

Fig. 4.—The section $\lambda\lambda$2235–2260 from LWP 31209, showing the richness of [Ne v] lines in this region. The rest wavelengths for [Ne v] were taken from Kurucz (1991); all others are from Kelly (1979). Most observed [Ne v] lines appear to be shifted shortward by about 0.2 Å. An echelle splice point is at 2262 Å, and reseau marks are at 2239 and 2256.5 Å.

TABLE 3

SUSPECTED EMISSION LINES IN THE CROWDED REGION $\lambda\lambda$1750–2870

λ(lab) (Å)	Ion (Multiplet)	Reference	Intensity[a]	λ(obs) (Å)	Comments
2755.11 + ...	O V (UV55)	1	8	2755.51	5 lines
2759.05	O IV	2	90	2759.19	
2767.50	Fe II	2	270	2768.13	2 lines, equal intensity
2777.71	C III (UV35)	2	110	2771.75	
2779.83	Mg I (UV6?)	2	160	2779.83	
2781.01	O V (UV32)	1	25	2781.57	Blend
2781.01	O V (UV32)	2	1000	2781.57	
2783.10	[Mg V]	2	...	2783.09	
2783.65	[Ar III]	2	50	2783.78	
2784.47	[Ar IV] (UV6)	2	120	2784.67	Blend
2783.23	[Ar III]	2	50	2785.67	
2785.29	[Ne III]	2	100	2785.43	
2785.99	[Ar V] (UV28)	2	...	2785.90	
2786.17	[Ne III]	2	40	2786.62	
2786.89	[Ne III]	2	60	2786.99	
2786.99	[O V]	2	920	2786.85	Blend
2786.99	[O V] (UV32)	1	24	2786.85	
2789.85	[O V] (UV32)	1	22	2789.28	Blend
2789.85	[O V] (UV32)	2	775	2789.28	
2795.52	[Mg II] (UV1)	2	400	2795.80	Interstellar absorption
2797.98	[Mg II] (UV3?)	2	350	2796.94	Interstellar absorption
2800.24	[Ne III]	2	60	reseau	
2802.34	[Ne III]	2	40	2802.26	
2802.69	[Mg II] (UV1)	2	300	2803.11	Interstellar absorption
2805.84	O IV	2	150	2805.95	
2854.50	[Ar IV]	2	...	2854.18	?
2869.00	[Ar IV]	2	...	2869.80	?

[a] Lab intensities from Moore 1993 and Kelly 1979 not on same scale.

REFERENCES.—(1) Moore 1993; (2) Kelly 1979.

cm^{-2} s^{-1} and nebular sum of 1.2×10^{-12} ergs cm^{-2} s^{-1} for the λ1909 component, resulting in the nebular log $N_e = 3.6 \pm 0.2$ cm^{-3}. Because of saturation, we are not able to deconvolve the C III] lines for SWP 55994 or SWP 55067. A value of log $N_e = 2.98$ cm^{-3} was determined by SKSD95 from the optical [S II] ratio.

Unusual as it is, the triple-peaked C III] $\lambda\lambda$1907, 1909 emission is not unique: a similar profile was observed in NGC 6751 (Feibelman 1995) and may also be present in NGC 5189 and NGC 2371-2 (in preparation), thus suggesting that such profiles may be characteristic of O VI–type W-C objects.

The Si III] λ1892 line is extremely weak in NGC 6905, so that the F(Si III])/F(C III]) diagnostic is unreliable for N_e from low-dispersion data.

From LWP 31209 we determine log $N_e = 3.9 \pm 0.1$ cm^{-3} for the fairly strong [Ne IV] $F(\lambda2425)/F\lambda2422)$ ratio, based on the diagnostic curves of Kafatos & Lynch (1980). We

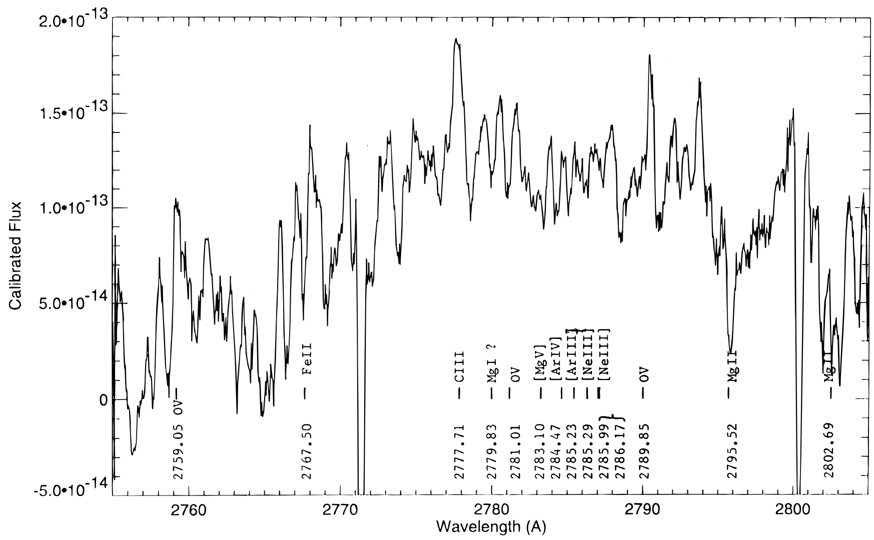

FIG. 5.—The region $\lambda\lambda$2755–2805 from LWP 31209. This condensed and smoothed plot shows numerous emission lines crowded into a small wavelength interval that makes identification uncertain. The *rest wavelengths* of some emission lines are indicated by tick marks. Moreover, it is difficult to ascertain the continuum level in this crowded region, thus making flux measurements of individual lines impossible. This region for NGC 6905 strongly resembles that of the spectrum of Sand 3.

TABLE 4

EMISSION FLUXES FROM HIGH-DISPERSION SPECTRA[a]

λ(obs) (Å)	λ(lab) (Å)	Ion	Reference	Flux (10^{-13} ergs cm^{-2} s^{-1})	Comments
			From Co-added SWP 18366, 55994, 56067		
1163.87	1164.08	O VIII?	1	4.47	
1164.59	1164.77	O VIII?	1	5.13	
1165.02	1165.37	O VIII?	1	1.04:	
1167.95	1168.99	C IV	2	18.72	3 peaks?
1170.02	1170.	?	...	4.58	
1172.14	1172.43	O VI	2	4.13	
1176.62	1175.50	C III	1	3.79	6 lines, UV4
1178.93	1178	?		6.73	
1184.23	1184.77	C IV	2	4.96	
1193.51	1193.	?		3.67	
1230.50	1230.04	C IV	2	0.54	
1230.64	1230.52	C IV	2	1.46	
1238.28	1238.82	N V	3	...	Interstellar absorption
1243.04	1242.80	N V	3	...	Interstellar absorption
1247.62	1247.55	C III	1	2.86	5 blended lines
1293.08	1293.30	[Mg V]	4	1.39	
1315.48	1315.85	C IV	1	1.15	
1325.31	1324.50	[Mg V]	4	2.45	
1440.51	1440.36	C IV	2	1.26	
1574.78	1574.80	[Ne V]	5	0.78	
1576.01	1576.55	C III	6	0.55	
1619.77	1619.80	C V	1	0.43	
1620.16	1620.33	C III	1	0.19	
1623.50	1623.63	O VII?	1	0.23	
1638.43	1638.30	O VII	1	0.69	
1722.12	1722.09	[Ne V]	5	0.43:	
1813.53	1814.60	[Ne III]	4	0.72	
			From SWP 18366 Only		
1907/09......	1907/09	C III]		...	See § 4.2.2
			From LWP 31209		
1930.56	1930.76	O VIII	1	1.56	
1932.58	1932.58	O VIII	1	3.32	
1979.34	1979	...		0.74	
1979.71	1979	...		1.09	Three lines; see text, § 3
1980.02	1980	...		1.06	
1982.89	1982.20	?		1.64	
1984.34	1984.59	C IV	2	1.38	
1980.55	1980.29	[Ne V]	6	...	
1989.55	1989.29	[Ne V]	5	2.25	See text, § 3
2068.75	2069.92	O VI	1	0.97	
2069.83	2070.29	O VI	1	1.10	
2222.79	2224.10	[Ne V]	5	1.05:	
2232.39	2232.79	[Ne V]	5	3.24	
2233.96	2233.59	[Ne V]	5	1.64	
2236.03	2236.29	[Ne V]	5	0.89	
2237.44	2237.57	Fe II	6	1.69	
2244.13	2245.50	Fe II	6	3.76	
2248.73	2249.88	[Ne V]	5	0.59:	
2250.16	2249.18	Fe II	6	1.93	
2252.05	2251.76	[Ne V]	5	1.59	
2253.43	2252.69	He II	6	3.37	
2257.01	2256.43	[Ne V]	5	0.87	
2259.28	2259.59	[Ne V]	5	1.42	
2263.66	2263.38	[Ne V]	5	0.64	
2264.22	2264.25	[Ne V]	5	0.95	
2265.22	2265.69	[Ne V]	5	0.95	
2267.23	2266.98	[Ne III]	6	0.94	
2270.07	2270.91	C V	1	0.64	Very weak
2272.94	...	?		1.43	
2273.34	2273.64	[Ne III]	6	4.18	
2277.38	2277.25	C V	1	1.35	
2277.74	2277.92	C V	1	1.14	
2282.45	2282.60	[Ne V]	5	1.38	
2297.16	2297.	C III	3	0.94	
2421.89	2422.50	[Ne IV]	4	3.91	
2424.46	2425.10	[Ne IV]	4	4.14	

TABLE 4—*Continued*

λ(obs) (Å)	λ(lab) (Å)	Ion	Reference	Flux (10^{-13} ergs cm^{-2} s^{-1})	Comments
2511.25......	2511.20	He II	6	0.87	
2523.25......	2523.70	C IV	1	0.37	
2530.09......	2529.98	C IV	1	0.28	
2533.12......	2233.77	C IV	1	0.33	
2733.13......	2733.29	He II	6	4.51	
2783.77......	2783.00	[Mg V]	4	0.24	
2784.8	2786.10	[Ar V]?	4	0.24	
2900.19......	2901.60	C IV	1	0.65	
2929.41......	2928.30	[Mg V]	4	0.56	
2969.68......	2970.20	[Ne V]?	6	0.62	
2974.67......	2974.29	[Ne V]	5	0.81	
2977.26......	2976.71	O VIII	7	0.59	
2979.13......	2979.85	Fe II?	6	0.80	
2980.43......	2980.60	[Ne V]	6	0.33	C V λ2980.97?
2993.51......	2992.90	[Ne V]	6	0.45	O V λ2993.0?
2995.14......	2995.20	[Ne V]	6	2.53	
2996.37......	2996.51	O III?	6	0.23	
2997.42......	2997.29	Fe II	6	0.38	
2998.46......	2998.43	N V?	6	0.30	
3001.58......	3001.58	Fe III	6	1.66	Strong doublet
3016.83......	3016.15	[Ar IV]?	6, 8	0.91	O III λ3017.63?
3020.80......	3021.07	Fe II?	6, 8	0.66	Si II λ3020.78?
3022.05......	3022.00	Fe III?	6, 8	0.52	Si II λ3021.55?
3023.63......	3024.36	O III	6	2.12	
3031.12......	30	?		1.21	
3047.23......	3047.13	O III	6	0.71	
3133.90......	3132.86	O III	6	>3.86	Affected by reseau
3203.08......	3203.10	He II	6	0.74	

[a] From well-resolved or isolated lines.

REFERENCES.—(1) Moore 1993; (2) Feibelman & Johansson 1995; (3) Morton 1991; (4) Mendoza 1983; (5) Kurucz 1991; (6) Kelly 1979; (7) Garcia & Mack 1965; (8) Adelman et al. 1977.

consider this to be a more accurate value than log $N_e = 5.4 \pm 0.2$ cm^{-3} derived from the low-dispersion $F(\lambda1601)/F(\lambda2422+2425)$ ratio and Nussbaumer's (1982) diagnostics, after the observed fluxes were corrected for $E(B-V) = 0.15$ adopted from B89. The weakness of the [Ne IV] λ1601 line and blend with C IV λ1595 adds to the uncertainty.

The N IV $F(\lambda1483)/F(\lambda1486)$ diagnostic cannot be applied to NGC 6905 because of the weakness of the N IV] lines.

A mean density of $N_e = 1100$ cm^{-3} is given by Pottasch (1984, p. 300) for $T_e = 12{,}000$ K.

In Table 5 we summarize some of these parameters taken from recent literature and from this work.

4.2.3. He II *Variability: Intrinsic or Position Angle?*

The He II λ1640 emission poses an interesting question. Comparison of the three high-dispersion SWP spectra indicates a real change in the emission profile and intensity as shown in Figure 8. Optical variability of λ4686/Hβ was shown by VV61 to have occurred between 1945 and 1959, thus providing a basis for labelling NGC 6905 as a variable

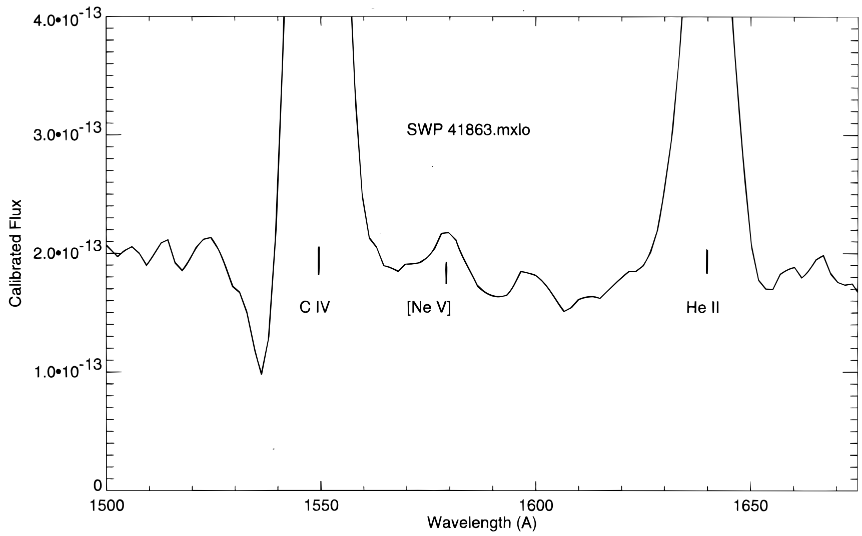

FIG. 6.—The P Cyg profile of the C IV λ1549 doublet from the low-dispersion spectrum SWP 41863, as discussed in § 4.2.1. The strong unsaturated C IV and He II emissions are shown here truncated for better visibility of the P Cyg absorption profile. The mean terminal wind velocity from three best spectra results in $V_\infty = -3880 \pm 200$ km s^{-1}. As in all other figures, the vertical scale is in units of ergs cm^{-1} s^{-1} $Å^{-1}$.

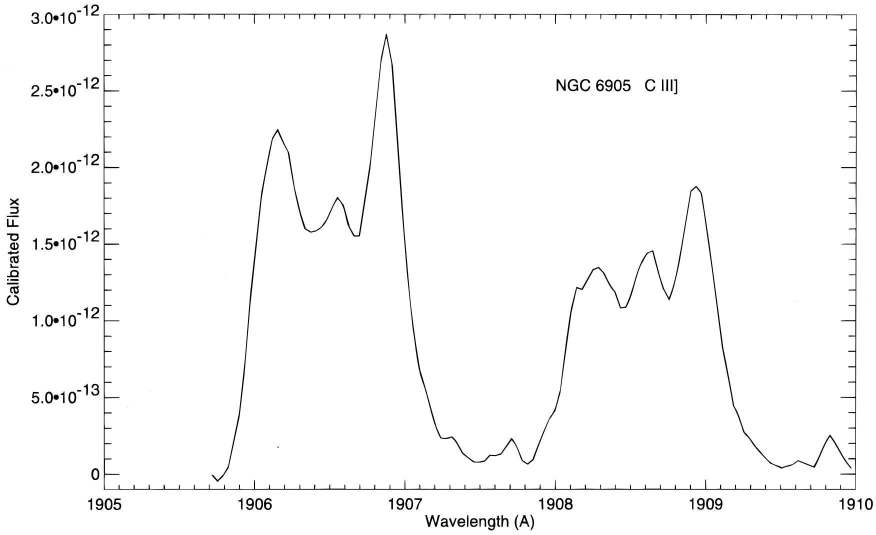

FIG. 7.—The C III] $\lambda\lambda$1907, 1909 lines as observed in the unsaturated high-dispersion spectrum SWP 18366. Each component consists of two nebular emissions and a central stellar component. These profiles were deconvolved into two sets of Gaussian components for determination of the stellar and nebular fluxes to yield the nebular log $N_e = 3.6 \pm 0.2$ cm^{-3}.

PN. The dual peak profile of the He II λ1640 line could be interpreted as the emission consisting of a stellar and a nebular component, or two nebular components. The change in the three spectra may be intrinsic or may be due to different angles of the major axis of the entrance aperture intercepting slightly different regions of the nebula.

We are not able to state unambiguously which one of these possibilities, or combinations of them, is responsible for the difference in line profile. The systemic radial velocity of NGC 6905 is given as -8.4 ± 1.7 km s^{-1} by A92 and as -10 km s^{-1} by SH82. This value lies near the trough of the two components of the He II λ1640.390 line for the three plots in Figure 8, in which the thin line represents SWP 18366, the thick one is for SWP 55994, and the medium one is for SWP 56067. Note that the deepest trough corresponds to neither the shortest (200 minutes) nor the longest (532 minutes) exposure. The position angles for these exposures were $-24°$, $-3°$, and $-16°$, respectively, and the deepest valley between the peaks corresponds to the smallest P.A., $-3°$. We interpret the two peaks as nebular emission rather than of stellar origin, as there is no peak near -10 km s^{-1}, but we cannot rule out some stellar contribution. This is, however, in contrast to the optical He II λ4686 line shown by Smith & Aller (1969), where a narrow nebular He II emission is superposed on a very broad stellar W-R emission. We should expect to see a strong stellar He II component, but this may be buried in the trough of the profile.

The nebular *expansion* velocity of 51.5 km s^{-1} is then determined from half the separation of the two peaks at 103 ± 5 km s^{-1}, in reasonable agreement with the expansion velocity of 47 km s^{-1} determined by SH82 from λ5007. From the C III] λ1907 and λ1909 profiles, we obtain a value of 55 km s^{-1}. Weinberger (1989) gives a weighted expansion velocity $2V_{\rm exp} = 87$ km s^{-1} from [O III] λ5007 and $2V_{\rm exp} = 73$ km s^{-1} from Hα, where the double expansion velocity was chosen following Sabadin (1984) to indicate real expansion as indicated by double-bowed appearance of lines, i.e., line splitting. When $2V_{\rm exp}$ versus $V_{\rm term}$ is added to Figure 1 of

TABLE 5

NGC 6905 PARAMETERS

Parameter	Value	Reference
$T_{\rm eff}$ (K)	104,000	1
$L^*/L_\odot$	3500	1
O VI $\lambda\lambda$3811, 3820 EW (Å)	700	1
Pulsation period (minutes)	16	2
$V_{\rm exp}$, [O III], mean (km s^{-1})	43.5	3
$V_{\rm exp}$, [O III] (km s^{-1})	47	4
$V_{\rm exp}$, He II (km s^{-1})	51.5	5
$V_{\rm exp}$, C III] (km s^{-1})	55.0	5
V_∞, C IV (km s^{-1})	-3880 ± 200	5 (see § 4.2.1)
V_∞, O V (km s^{-1})	-2730 ± 150	5 (see § 4.2.1)
log N_e, [S II] (cm^{-3})	2.98	1
log N_e, C III] (cm^{-3})	3.6 ± 0.2	5
log N_e, [Ne IV] (cm^{-3})	3.9 ± 0.1	5
log N_e, mean (cm^{-3})	3.1	6

[a] Several modes.

REFERENCES.—(1) Kaler & Shaw 1984; (2) Bond & Ciardullo 1990, 1993; (3) Weinberger 1989; (4) Sabbadin & Hamzaoglu 1982; (5) this paper; (6) Pottasch 1984.

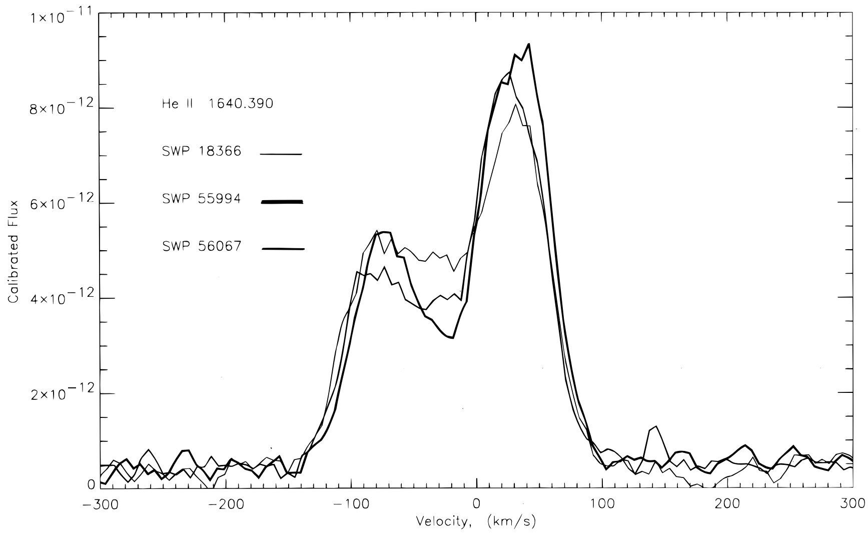

FIG. 8.—Multiplot of the He II λ1640.390 emission line in velocity space from three SWP high-resolution spectra, SWP 18366 (*thin line*), 55994 (*thick line*), and 56067 (*medium line*). The large entrance aperture was in position angle $-3°$, $-16°$, and $-24°$, respectively, for these exposures. Notice that the deepest trough and highest amplitude is for SWP 55994.

PP91, NGC 6905 falls near the end of their straight line empirical relation,

$$V_{\rm edge} = 91\ V_{\rm exp} + 157\ ({\rm km\ s^{-1}})\ ,$$

for both quantities of values shown by PP91.

We note that the He II λ4686 and λ5412 emissions shown by CPM93 (in their Fig. 11) display a split profile similar to that of the λ1640 feature.

A multiplot of the strongest He II lines observed in LWP 31209, $\lambda\lambda$3203, 2733, 2511, is shown in velocity space in Figure 9. The profiles for λ2733 and λ3203 are double peaked, as was noted earlier for λ2734 by F82 from low-dispersion line-by-line analysis. However, when λ3203 (or $\lambda\lambda$2511, 2733) is compared with the λ1640.39 line from SWP 55994, they appear to be shifted because different portions of the nebula are seen in SWP and LWP, as indicated by their respective P.A., $-3°$ and $+63°$.

As Table 1 shows, the position angle (P.A.) of the major axis of the entrance aperture varies strongly for the different exposures. The range of P.A. for the SWP high-dispersion spectra differs by only 21° (from $-3°$ to $-24°$), but the LWP 31209 P.A. at $+63°$ is nearly orthogonal to the SWP spectra and may explain the difference of line profiles seen in He II λ1640 compared to those of He II $\lambda\lambda$2511, 2733, 3203.

4.2.4. *Is there* O VIII *Emission Present?*

Very high excitation lines, such as O VIII (IP = 871.4 eV) λ6068 ($n = 10 \rightarrow 9$) and λ4340 ($n = 9 \rightarrow 8$) have been confirmed in the very hot helium-rich white dwarf KPD 0005+5106 by Werner, Heber, & Fleming (1994), as well as in some central stars of planetary nebulae (CSPNs), and they are thought to be of coronal origin. Coronal winds were also suggested by Hartmann & Raymond (1978) for O VI emission observed in early stars as well as the central

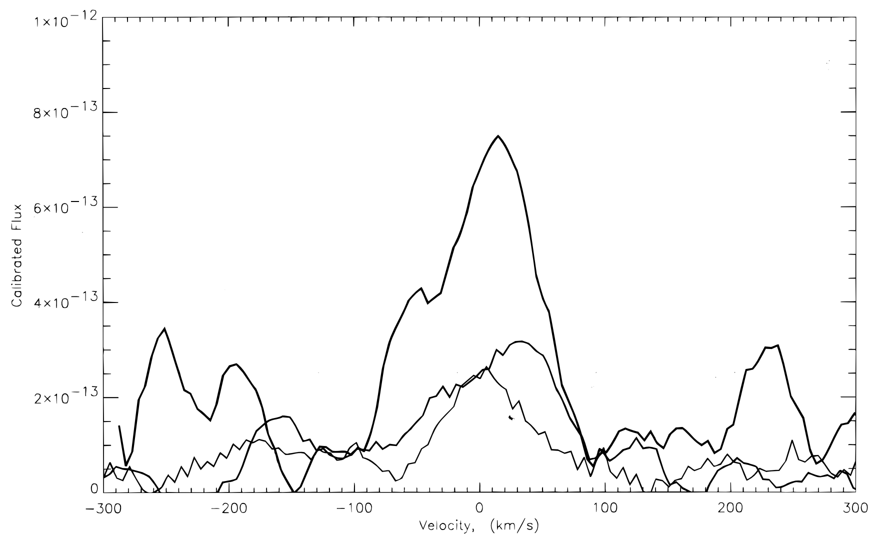

FIG. 9.—Multiplot of the He II emission lines $\lambda\lambda$2511 (*thin line*), 2733 (*medium line*), and 3203 (*thick line*) from LWP 31209 in velocity space. All tracings are to the same scale shown at left.

stars of NGC 6905 and NGC 6751. For KPD 0005+5106, the $\lambda4340$ emission is coincident with Hγ in absorption. However, corresponding O VIII emissions near $\lambda1930$ and $\lambda2976$ have been observed. We have no definite optical identification of O VIII for NGC 6905, but there are hints that O VIII at 6068 Å may be present: Aller (1977) lists an unidentified broad feature at $\lambda\lambda6057$–6085; moreover, Johnson (1976) also lists an unidentified weak stellar emission at $\lambda6064$. The recent line list by SKSD95 unfortunately does not show any lines longward of $\lambda5876$ for NGC 6905; however, the Balmer decrement agrees very well for I(Hγ) with the predicted value (Aller 1984) for $T_e = 10^4$ K and log $N_e = 3$ cm^{-3}, thus probably leaving no room for O VIII $\lambda4340$ emission, unless it is very weak.

4.2.5. O VIII *Emission Lines in the UV*

Because of the similarity of the optical and UV spectra of NGC 6905 and the very hot, ultra–high excitation star Sanduleak 3 (which is definitely known to have O VIII as well as O VII lines in the optical spectrum; BH82, Barlow, Blades, & Hummer 1980), it is tempting to search for O VIII emission lines in the *IUE* spectra of NGC 6905. The *IUE* low-dispersion ($\delta\lambda/\lambda = 7$ Å) SWP 41863, 16703, and 14401 spectra show a weak emission near $\lambda1930$ that *may* be due to O VIII emission, as seen in Figure 1. In SWP high-dispersion spectra, the O VIII doublet, $\lambda\lambda1930.763$, 1932.853, falls into a region of the echelle spectrum near an interorder gap, thus making positive identification difficult. Fortunately, there are no gaps in the LWP high-dispersion region near $\lambda1930$, but here the sensitivity is low, thus requiring very deep exposures. The 488 minute LWP 31209 is adequate in this respect and shows a pair of emissions that are broader than the random noise pattern, with a separation of 2.02 Å that corresponds almost exactly to the separation given by M93. They are thought to be due to the O VIII doublet at $\lambda1930.763$ and $\lambda1932.853$, multiplet UV94, $\delta\lambda = 2.09$ Å (M93), shown in Figure 10 that covers the region of 1928–1934 Å. The $\lambda1930$ feature is also seen in the SWP range but the $\lambda1932$ line is unobservable, as it falls into the echelle interorder gap mentioned above.

Additional O VIII transitions are listed by M93 near $\lambda\lambda1164$, 1165, 1170, and 1171. We were able to detect the first pair but not the second.

Another line near 2977 Å is detectable at high resolution and may represent a mixture of [Ne V] and the O VIII $\lambda2976.57$ line given by Garcia & Mack (1965) that was observed by Werner et al. (1996) in *Hubble Space Telescope* (HST) data of RX J2117+3412 and KPD 0005+5106. Figure 11 shows the *IUE* region $\lambda\lambda2968$–2978. These features need to be reobserved at higher S/N than is presently possible with *IUE*.

4.2.6. *The* O VII *Triplet*

The only O VII feature observable in the *IUE* wavelength range is the triplet $\lambda\lambda1623.63$, 1638.30, 1639.87 (multiplet 8) given in M93. Of the three transitions, only the $\lambda1638$ emission is identified tentatively in the co-added SWP spectrum shown in Figure 12. This feature was also observed by F96a in *IUE* spectra of two other O VI PNs, NGC 2371-2 and NGC 5189.

4.3. *Variability in the UV Spectra*

Except for the peculiar difference in the He II $\lambda1640$ high-dispersion profiles that may be a function of position angle as described in § 4.2.3, emission lines from low-resolution spectra show remarkably little variability: each of the strong emission lines of O V $\lambda1371$, C IV $\lambda1549$, He II $\lambda1640$, and C III] $\lambda1909$ shown in Table 2 shows less than 5% variation during the years 1981–1991. A possible exception may be indicated by SWP 16703, which was taken under high background radiation conditions. In this spectrum, almost all the weaker lines are stronger than corresponding lines in the other three spectra.

We assign little importance to the lines below $\lambda1200$ and show the C IV $\lambda1168$ emission in parentheses to indicate low sensitivity and large errors.

If we are to look for variability, it may be found in the much weaker lines, notably those of C IV and O VI, but the errors are quite large ($\pm$ 50%) for these fluxes. Neverthe-

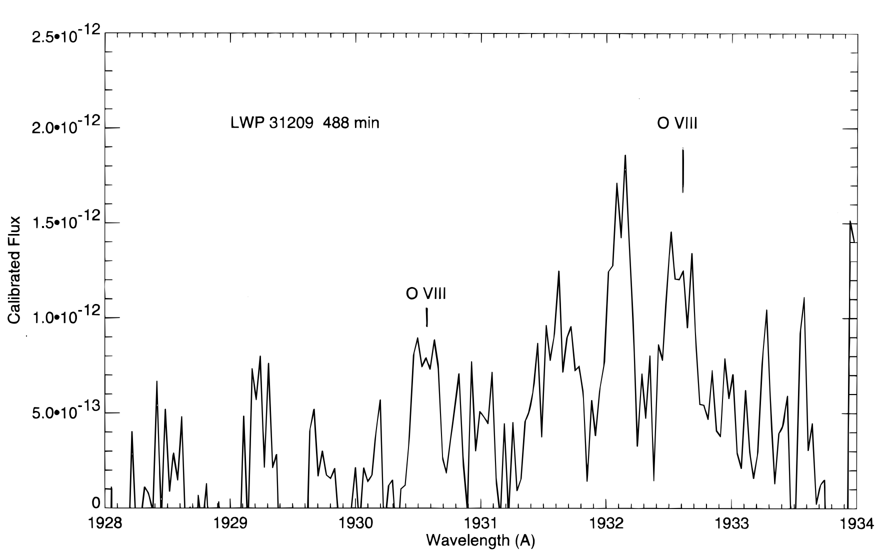

FIG. 10.—The region $\lambda\lambda1928$–1934 from LWP 31209 showing the O VIII doublet at $\lambda\lambda1930.763$, 1932.853, multiplet UV94. The observed separation of the two components is 2.02 Å and is almost exactly that of the lab wavelengths, $\delta\lambda = 2.09$ Å. The O VIII features are considerably broader than the random noise spikes.

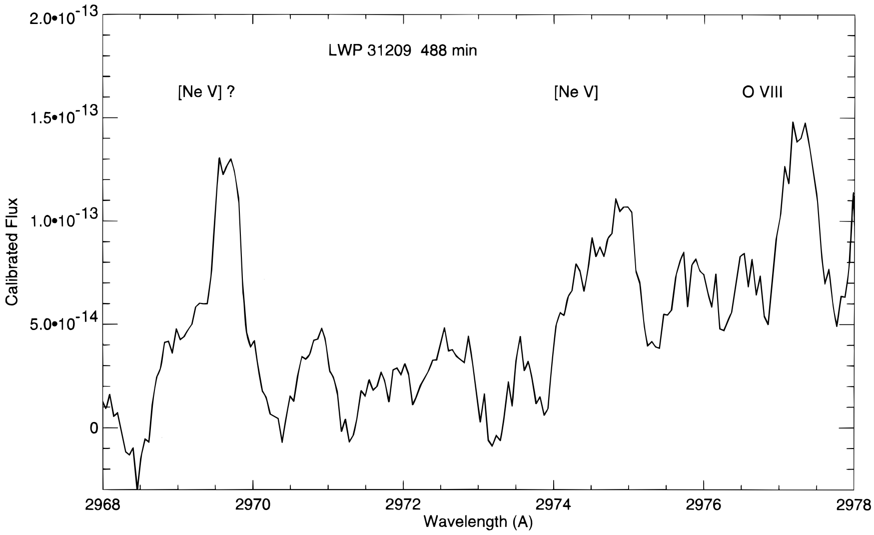

FIG. 11.—The region $\lambda\lambda$2968–2978 from LWP 31209, suggesting that emission lines of O VIII λ2976.57 and [Ne V] λ2974.20 are present. The third feature may represent [Ne V] λ2970.20 listed in Kelly (1979), although it is not listed in Kurucz (1991).

less, they may be indicative of PG 1159–type fluctuations or coronal winds that require further study.

4.4. *A New* "O VIII *Sequence*" *for PNs*

We conclude on a speculative note. The detection of O VIII emission lines in the *IUE* spectrum of NGC 6905 raises the question of whether there exists an "O VIII sequence" of PNs. At least two other CSPNs are definitely known to exhibit O VIII lines at optical and UV wavelengths. They are Sand 3 and the very hot X-ray source RX J2117+3412. As might be suspected, all three are also definite members of another small subset, namely, nonradial pulsating stars (Ciardullo & Bond 1996; Bond et al. 1993). Several other CSPNs are currently under investigation for O VIII emission in *IUE* spectra. Preliminary results indicate that NGC 2371-2, NGC 2867, NGC 5189, and NGC 5315 show O VIII emission. The first two definitely are pulsators, but NGC 5315 is not thought to be a pulsator by Ciardullo & Bond (1996).

After this paper was submitted, the existence of the "O VIII sequence" was confirmed from UV and optical data for a total of 10 PNs (Feibelman 1996b, hereafter F96b).

5. SUMMARY AND RECOMMENDATIONS

Although NGC 6905 has been known to show variability in optical spectra, no variability was detected in O V, C IV, He II and C III] from low-resolution data between 1981 and 1991. In fact, these lines were found to be remarkably stable, to $\pm 5\%$, after the data were reextracted by the latest reduction routines. Variations in the He II λ1640 line profile from high-resolution data may be intrinsic or a function of position angle of the major axis of the large entrance aperture.

Some variability may be present in weaker lines of C IV and O VI, possibly indicative of PG 1159–type activity, but these lines are an order of magnitude fainter than the strong emissions mentioned above and may have large errors ($\pm 50\%$). N V is very weak, if present at all. Long-term

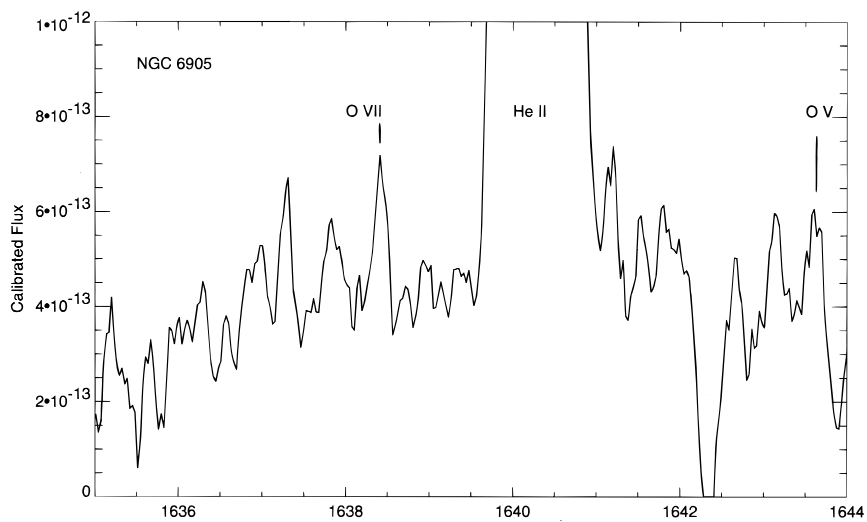

FIG. 12.—The region of the putative O VII emission at λ1638.30. This feature is present on the three individual spectra and this co-added plot. The very strong He II λ1640 line is truncated in this plot, which also shows the O V λ1643 emission.

monitoring of the optical O VI doublet near 3820 Å and other lines may be worthwhile to detect periodic spectral variations.

Electron densities were determined as log $N_e = 3.6 \pm 0.2$ cm^{-3} from deconvolved nebular components of C III] $F(\lambda1907)/F(\lambda1909)$, and log $N_e = 3.9 \pm 0.1$ cm^{-3} from [Ne IV] $F(\lambda2425)/F(\lambda2422)$.

NGC 6905 displays one of the highest ratios of $2V_{\rm exp}$ versus $V_{\rm edge}$ for any PN when added to the plot of Patriarchi & Perinotto (1991).

A terminal wind velocity of -3880 ± 200 km s^{-1} for C IV λ1549 was derived from the mean of the three best low-dispersion spectra, and a value of 2730 ± 150 km s^{-1} for the O V λ1371 line from three exposure-weighted co-added high-dispersion spectra.

Emission lines of O VIII at 1930, 1932, and 2977 Å were detected in the *IUE* spectra of NGC 6905, and possibly O VII near 1623 and 1638 Å, but these need to be confirmed by higher S/N spectra and by their optical counterparts.

Other high-excitation lines of C IV, C V, O VI, [Ar IV], and [Mg V] were observed. The strong optical lines of [Ne III] observed by SKSD95 are duplicated in the UV spectrum. In addition, strong [Ne IV] and numerous [Ne V] lines are observed, suggesting that NGC 6905 is a neon-rich object.

Preliminary results indicate O VIII emission lines also in the *IUE* spectra of NGC 2371-2, NGC 2867, NGC 5189, and NGC 5315, plus definite O VIII lines in RX J2117+3412 and Sand 3, suggesting that these objects represent a new "O VIII sequence" of planetary nebulae, as was recently confirmed by F96b.

It should be worthwhile to look for optical O VIII λ6068 emission and to search for X-ray emission from NGC 6905.

I thank the Goddard *IUE* staff for obtaining the 1995 spectra under the Service Observing program, and the VILSPA team for the SWP 56067 spectrum obtained during the 19th year episode of *IUE* operations for program SA018.

REFERENCES

Acker, A., et al. 1992, Catalog of Galactic Planetary Nebulae (Strasbourg: ESO) (A92)
Adelman, C. J., Adelman, S. J., & Fischel, D. 1977, NASA-X-685-77-287 (Washington, DC: NASA)
Aller, L. H. 1951, ApJ, 113, 139 (A51)
———. 1968, in IAU Symp. 34, Planetary Nebulae, ed. D. E. Osterbrock & C. R. O'Dell (Dordrecht: Reidel), 339 (A68)
———. 1977, JRASC, 71, 67
———. 1984, Physics of Thermal Gaseous Nebulae (Dordrecht: Reidel)
Balick, B. 1987, AJ, 94, 671
Barlow, M. J., Blades, J. C., & Hummer, D. G. 1980, ApJ, 241, L27
Barlow, M. J., & Hummer, D. G. 1982, in Wolf-Rayet Stars: Observations, Physics, Evolution, ed. C. W. H. de Loore & A. J. Willis (Dordrecht: Reidel), 387 (BH82)
Bianchi, L. 1989, in a Decade of UV Astronomy with *IUE*, ed. E. J. Rolfe (ESA SP-281, Vol. 2), 173 (B89)
Bond, H. E., & Ciardullo, R. 1990, in ASP Conf. Ser. 11, Confrontation Between Stellar Pulsations and Evolution, ed. C. Cacciari & G. Clementi (San Francisco: ASP), 529
———. 1993, in IAU Symp. 155, Planetary Nebulae, ed. A. Acker & R. Weinberger (Dordrecht: Kluwer), 489
Bond, H. E., Ciardullo, R., & Kawaler, S. D. 1993, Acta Astron., 43, 425
Chu, Y.-H., Jacoby, G. H., & Arendt, R. 1987, ApJS, 64, 529
Ciardullo, R., & Bond, H. E. 1996, AJ, 111, 3223
Cuesta, L., Phillips, J. P., & Mampaso, A. 1993, A&A, 267, 199 (CPM93)
Curtis, H. D. 1918, Publ. Lick Obs., Vol. 13
D'Odorico, S., Rubin, V. C., & Ford, W. K. 1973, A&A, 22, 469
Doschek, G. A., & Feibelman, W. A. 1993, ApJS, 87, 331 (DF93)
Feibelman, W. A. 1982, ApJ, 258, 562 (F82)
———. 1994, PASP, 106, 756
———. 1995, ApJ, 448, 766
———. 1996a, ApJ, 464, 910 (F96a)
———. 1996b, PASP, 108, 664 (F96b)
Feibelman, W. A., & Johansson, S. 1995, ApJS, 100, 405 (FJ95)
Garcia, J. D., & Mack, J. E. 1965, J. Opt. Soc. Am., 55, 654
Hartmann, L., & Raymond, J. C. 1978, ApJ, 222, 541
IUE Newsletter. 1992, 47, 25 (Washington, DC: NASA)
———. 1996, 56, in press
Johnson, H. M. 1976, ApJ, 208, 127
———. 1981, ApJ, 250, 590 (J81)
Kafatos, M., & Lynch, J. P. 1980, ApJS, 42, 611
Kaler, J. B., & Shaw, R. A. 1984, ApJ, 278, 195 (KS84)
Keenan, F. P., Feibelman, W. A., & Berrington, 1992, ApJ, 389, 443
Kelly, R. L. 1979, Atomic Emission Lines in the Near Ultraviolet, Section II (Washington, DC: NASA) (K79)
Kurucz, R. L. 1991, in NATO ASI Ser. C152, Stellar Atmospheres: Beyond Classical Models, ed. L. Crivellary, I. Hubeny, & D. G. Hummer (Dordrecht: Kluwer), 441
Louise, R. 1982, A&A, 114, 205
Louise, R., & Hua, C. T. 1984, Ap&SS, 105, 139
Mendoza, C. 1983, in IAU Symp. 103, Planetary Nebulae, ed. D. R. Flower (Dordrecht: Reidel), 143
Moore, C. E. 1993, Tables of Spectra of H, C, N, and O Atoms and Ions (Boca Raton: CRC Press) (M93)
Morton, D. C. 1991, ApJS, 77, 119 (M91)
Nichols, J. S., & Linsky, J. L. 1996, AJ, 111, 517
Nussbaumer, H. 1982, in The Nature of Symbiotic Stars, ed. M. Friedjung & R. Viotti (Dordrecht: Reidel), 85
Patriarchi, P., & Perinotto, M. 1991, A&AS, 91, 325 (PP91)
Phillips, J. P., & Mampaso, A. 1989, in IAU Symp. 131, Planetary Nebulae, ed. S. Torres-Peimbert (Dordrecht: Kluwer), 194 (PM89)
Pottasch, S. R. 1984, Planetary Nebulae (Dordrecht: Reidel)
Pottasch, S. R., Preite-Martinez, A., Olnon, F. M., & Jing-Er, M. 1986, A&A, 161, 363
Sabbadin, F. 1984, A&AS, 58, 273
Sabbadin, F., & Hamzaoglu, E. 1982, A&AS, 50, 1 (SH82)
Schneider, S. E., Terzian, Y., Purgathofer, A., & Perinotto, M. 1983, ApJS, 52, 399
Silvotti, R., Bartolini, C., Boffi, F. R., Cosentino, G., Guarnieri, A., Piccioni, A., & Stanghellini, L. 1993, in IAU Symp. 155, Planetary Nebulae, ed. A. Acker & R. Weinberger (Dordrecht: Kluwer), 491
Smith, L. F., & Aller, L. H. 1969, ApJ, 157, 1245
Stanghellini, L., Kaler, J. B., Shaw, R. A., & di Serego Alighieri, S. 1995, A&A, 302, 211 (SKSD95)
Swings, P., & Swensson, J. W. 1952, Ann. d'Astrophys., 15, 290
Tarafdar, S. P., & Apparao, K. M. 1988, ApJ, 327, 342
Vorontsov-Velyaminov, B. A. 1961, Soviet Astron.—AJ, 5, 186 (VV61)
Weinberger, R. 1989, A&AS, 78, 301
Werner, K., Dreizler, S., Heber, U., Rauch, Fleming, T. A., Sion, & Vauclair, G. 1996, preprint
Werner, K., Heber, U., & Fleming, T. A. 1994, A&A, 284, 907